Turkish Journal of Electrical Engineering & Computer Sciences

http://journals.tubitak.gov.tr/elektrik/

Research Article

Turk J Elec Eng & Comp Sci
(2017) 25: 3854 – 3867

doi:10.3906/elk-1606-461

Fault location in distribution systems with DG based on similarity of fault impedance

Zahra MORAVEJ[1,*], **Omid HAJIHOSSEINI**[1], **Mohammad PAZOKI**[2]
[1]Faculty of Electrical & Computer Engineering, Semnan University, Semnan, Iran
[2]School of Engineering, Damghan University, Damghan, Iran

Received: 28.06.2016 • **Accepted/Published Online:** 20.06.2017 • **Final Version:** 05.10.2017

Abstract: This paper presents a new method for locating a fault in distribution systems using the similarity of fault impedance. A four-step approach is proposed to locate the fault in the networks. First, pre- and during-fault voltages from smart feeders along the primary feeders are measured. Second, three-phase impedance to calculate fault current corresponding to voltage deviation from each smart meter is achieved. Third, a relation between fault current and fault impedance for each type of fault is extracted. Finally, based on the similarity of the estimated fault impedance for each bus, an error index is calculated. Moreover, an auxiliary process is utilized to analyze the estimated fault impedance. The proposed method uses both smart meters and phasor measurement units to obtain voltage sag. Distributed generation and loads are modeled as constant impedances and then they are considered in the three-phase impedance matrix. The suggested approach is evaluated in the IEEE 34-bus test distribution network, which is simulated in the PSCAD/EMTDC environment. The obtained numerical results confirm the acceptable accuracy of the proposed methodology for all types of faults with various fault resistances.

Key words: Phasor measurement units, distributed generation, fault impedance, distribution system, three-phase impedance matrix, voltage sags

1. Introduction

Knowledge of fault location with maximum accuracy and minimum time can speed up system restoration and repair processes. Distribution systems with distributed generations (DG) and renewable energy resources will have a key role in continuous load support in future networks. Moreover, disconnecting them in fault conditions may make the system unreliable and cause problems such as island operation in fault cases [1[]. Fault location is presented as a challenging task in promoting repair and restoration of faulted transmission lines and distribution feeders [2]. Repair and restoration procedures need the faulted bus location in distribution networks.

Traditionally, fault location methods were based on the operator's experience and trial and error in reconfiguring power switches in a network. With propagation call centers, customer's calls come to help operators to find the estimated location of a fault. Recently, computer-based methods have been introduced to speed up fault location and avoid extra stress to the equipment during the switching on and off of a section. Recently, different fault location methods have been introduced. Fault location algorithms can be categorized according to input data [2]:

1. apparent impedance measurement,

*Correspondence: zmoravej@semnan.ac.ir

2. direct three-phase circuit analysis,
3. superimposed components,
4. traveling waves,
5. power quality monitoring data,
6. artificial intelligence.

In [3,4], the apparent impedance, which is determined as the ratio of voltage to current in the selected line based on the fault type, was calculated for every line in the network. In addition to measuring voltage and current at a substation, the network electrical parameters were used to examine the apparent impedance at all lines in the network. Multiple estimation existing in fault locations results due to measuring of voltage and current only at the substation. Moreover, fault resistance affects the performance of these methods. In [4], by the increase of phasor measurement units (PMUs), the problem of multiple fault location estimation was solved.

The methods based on traveling waves need high sampling frequency, which increases the implementation cost. Due to presence of many laterals and transformers in a distribution system, the traveling waves will be reflected. Consequently, confused results will be obtained. The traveling wave-based methodologies are suitable for transmission lines [5,6].

In [7], by defining the network as multiple sections and using a decision tree (DT), the fault location accuracy was improved. Moreover, the DT reduced the computational complexity. In [8], matching pursuit decomposition was utilized for feature extraction from voltage signals. Then a hybrid-clustering algorithm was used to cluster some specific vectors for fault location purposes. Artificial intelligence-based methods need a huge number of training data, as well as requiring a retraining procedure through change in network topology.

Voltage sag monitoring is an efficient and cheap way to locate faults in distribution networks. In [9], voltage sag data collected from intelligent electronic devices were utilized. Accordingly, the method used the 2n+1 point estimation method to calculate the statistical moment. Moreover, Chebyshev's inequality was provided for ranking these moments to locate the faulted bus in the network. In [10], a fault distance equation based on a trigonometric relationship of measured and simulated voltage sag and current magnitudes was formulated. In each candidate for faulted sections, the proposed algorithm in [15] returned two values of fault distance because of positive and negative measurement errors. Furthermore, for multiple fault sections, a ranking approach was utilized. In [11], based on comprehensive sensing, the fault current vector from a limited number of voltage sag meters was recovered. The performance of this algorithm was improved in [12]. In [12], nonzero values in the current vector by fuzzy c-mean clustering to estimate four possible faulted points was examined. In addition, a machine learning technique based on the k-nearest neighbor was applied in single-phase faults. In [13], the proposed method used smart meters to measure voltage sag and then calculated the fault current based on the impedance matrix. Moreover, the automated outage mapping enhanced the performance of the method by reducing the multiple estimations.

Multiple fault locations are one of the remarkable problems of voltage sag-based methods. In this paper, fault impedance as an efficient factor to improve the performance of voltage sag-based methods in multiple estimations is proposed. Moreover, an effective methodology for faulted bus locations, which has acceptable accuracy for different fault conditions in distribution systems with DG units, is discussed. In addition, the proposed algorithm is applicable in single-phase feeders for the purpose of fault location. Section 2 presents

the theoretical formula of the method. Sections 3 and 4 provide simulation results and discussion, respectively. The paper is concluded in Section 5.

2. Formulation of proposed methodology

The proposed algorithm is developed based on short-circuit theory and Thevenin's theorem. The flowchart of the proposed method is shown in Figure 1. Backward/forward sweep load flow are utilized to calculate prefault feeder voltages in the network [14]. PMUs and smart meters are categorized as smart measurement devices. Smart measurement devices report outages and measured voltage sags in the fault conditions. PMUs are utilized to measure the magnitude and phase of deviation voltage along the feeders, whereas smart meters are used just for measuring the voltage magnitudes [11]. When a fault occurs in the feeder, each node has specific voltage sag with different magnitudes and phase angles [15]. These voltage sags are utilized to estimate a fault current of each feeder by short-circuit theory. Then, according to Thevenin's theorem, fault impedance is calculated corresponding to each meter of every bus in the network. Finally, the similarity of the fault impedance index and auxiliary process is used to detect the faulted bus.

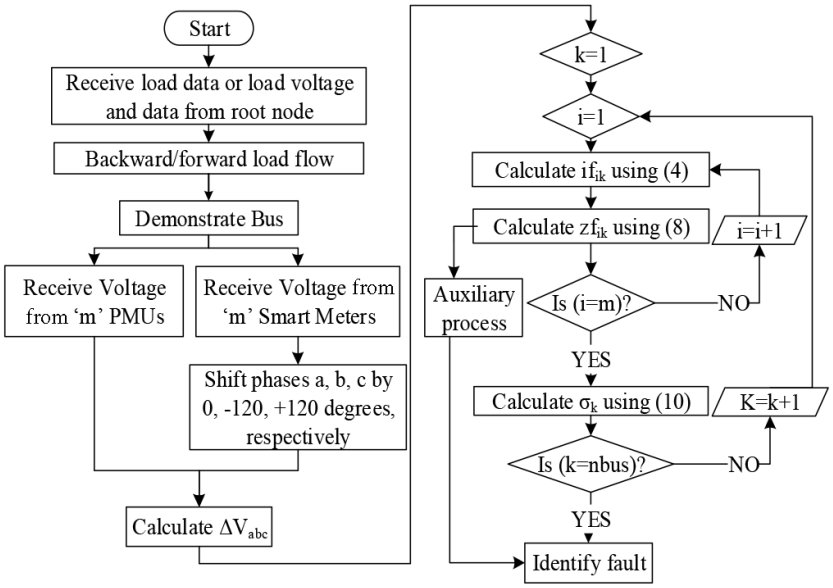

Figure 1. The proposed flowchart to identify the faulted bus.

2.1. Zbus calculation

The proposed method covers considerable issues in distribution networks such as load taps, existence of lateral, unbalanced lines, and DG. In this section, loads, lines, and DG are modeled.

Thevenin's equivalent circuits of each source are extracted and included in the impedance matrix. In the proposed method, positive, negative, and zero sequence impedances of distributed generators are used to demonstrate the equivalent impedance matrix. Figure 2 illustrates the conventional notation of these models [16]. When a fault occurs at the terminal of DG, according to Figure 2, sequence impedance is calculated as in [17]. According to the symmetrical component, sequence impedance is converted to three-phase impedance by:

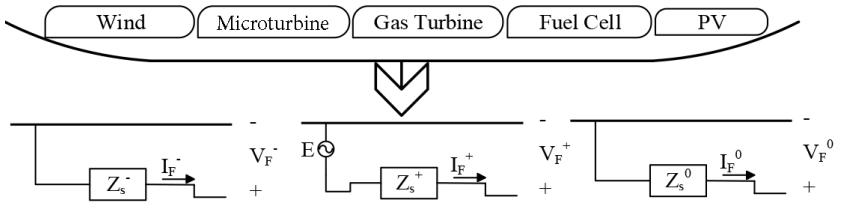

Figure 2. Thevenins equivalent of DG units.

$$Z_{abc} = \left(\begin{pmatrix} 1 & 1 & 1 \\ 1 & a^2 & a \\ 1 & a & a^2 \end{pmatrix} \right)^{-1} \times Z_{012} \times \begin{pmatrix} 1 & 1 & 1 \\ 1 & a^2 & a \\ 1 & a & a^2 \end{pmatrix}, \; a = e^{\frac{i2\pi}{3}}. \tag{1}$$

This procedure returns the accurate source impedance that is modeled into a three-phase impedance matrix irrespective of the DG type or its interface.

The loads and capacitors are represented as constant impedance and they are included in the impedance matrix. Information of the customer's power meter is used to estimate load impedance. If load type, nominal voltage, and power of load are given, there is a straightforward process to calculate the load impedance, which is used in this paper. The loads in the distribution system are specified on their nominal complex power demand. Load power is calculated by measuring RMS voltage as:

$$S = \alpha \times S^{nom} + \beta \times S^{nom} \times \left(\frac{|V|}{|V_{nom}|} \right) + \gamma \times S^{nom} \times \left(\frac{|V|}{|V_{nom}|} \right)^2, \tag{2}$$

where α is the ratio of constant power load, β is the ratio of constant current load, γ is the ratio of constant impedance load, and $\alpha + \beta + \gamma = 1.0$.

Although the load impedance values are calculated either from Eq. (2) or load curves, information of load curves or load voltages must be updated before construction of the three-phase impedance matrix. When complex power of the load is determined, the impedance matrix of each load is calculated as described in [18]. There are six types of loads (constant impedance, power, and current loads in wye and delta group) that have been modeled in this paper.

Unbalanced distribution lines are described by the impedance and susceptance matrix. A pi-section is primarily used to represent an overhead line or underground cable since this representation will provide the correct fundamental frequency impedance. When the network topology, line, and load data are known, the three-phase impedance matrix is determined [19].

2.2. Fault current calculation

According to the proposed method in [20], the voltage deviation $\Delta V_{3n\times1}$ due to fault current is given by:

$$\Delta V_{3n\times1} Zbus_{3n\times3n} \times If_{3n\times1} \tag{3}$$

where $If_{3n\times1}$ is the fault current vector and $Zbus_{3n\times3n}$ is the three-phase impedance matrix for the n bus distribution system. If a fault occurs only in bus k, the fault current vector has three nonzero elements and

Eq. (3) is rewritten as:

$$\begin{bmatrix} If_a \\ If_b \\ If_c \end{bmatrix}^{k}_{3\times1} = \left(\begin{bmatrix} Z_{aa} & Z_{ab} & Z_{ac} \\ Z_{ba} & Z_{bb} & Z_{bc} \\ Z_{ca} & Z_{cb} & Z_{cc} \end{bmatrix}^{k}_{3\times3} \right)^{-1} \times \begin{bmatrix} \Delta V_a \\ \Delta V_b \\ \Delta V_c \end{bmatrix}^{i}_{3\times1} \tag{4}$$

where $If_{3n\times1}$ is estimated fault current on bus k due to voltage sag and $\Delta V^i_{3\times i}$ on bus i. When there are single- or double-phase feeders, mutual impedance, $Zbus^{ik}_{3\times3}$, is singular. Therefore, Eq. (4) is inapplicable for fault current calculation.

In single-phase feeders, if both bus k and bus i are single-phase feeders, then $Zbus^{ik}_{3\times3}$ has only one nonzero element. There is one equation and one variable. In a single-phase-to-ground fault (AG), fault equation (a) in Eq. (5) is approved, and then $If^k_{3\times1}$ is obtained. When i is a three-phase feeder, there are three equations and one variable as follows:

$$\begin{cases} (a): \Delta V^i_a = Z^{ik}_{aa} \times If^k_a \\ (b): \Delta V^i_b = Z^{ik}_{ba} \times If^k_a \\ (c): \Delta V^i_c = Z^{ik}_{ca} \times If^k_a \end{cases} \tag{5}$$

Simulation results show that the proposed method has satisfying performance when voltage deviation is utilized for the same faulty phase.

In two-phase feeders, the same approach is utilized. For a double-phase-to-ground fault (ABG), the fault current is calculated as:

$$\begin{bmatrix} If^k_a \\ If^k_b \end{bmatrix} = \left(\begin{bmatrix} Z_{aa} & Z_{ab} \\ Z_{ba} & Z_{bb} \end{bmatrix}^{-1} \right) \times \begin{bmatrix} \Delta V^i_a \\ \Delta V^i_b \end{bmatrix} \tag{6}$$

Therefore, if there are m smart measurement devices in the network then there are m estimated fault currents of each favorite bus. For example, in bus k:

$$bus(k) = \left\{ If^1_{3\times1}, If^2_{3\times1}, \cdots If^m_{3\times1} \right\} \tag{7}$$

2.3. Fault impedance calculation

The fault impedance is considered as network n1 and the distribution system as network $n2$. Thevenins equivalent circuits n1 and n2 are shown in Figure 3. Applying KVL to route R, the following voltage equation is obtained:

$$-Vf^{k\_pre-fault}_{3\times1} + Zth^k_{3\times3} \times If^k_{3\times1} + Zf^k_{3\times3} \times If^k_{3\times1} = 0 \tag{8}$$

where $Vf^{k\_pre-fault}_{3\times1}$ is the bus k prefault voltage bus that is calculated by backward/forward load flow [14]. $Zth^k_{3\times1}$ is equivalent impedance from the three-phase impedance matrix, and is fault impedance. Corresponding different fault types are as shown in Figure 4. Accordingly, the fault impedance is calculated as follows:

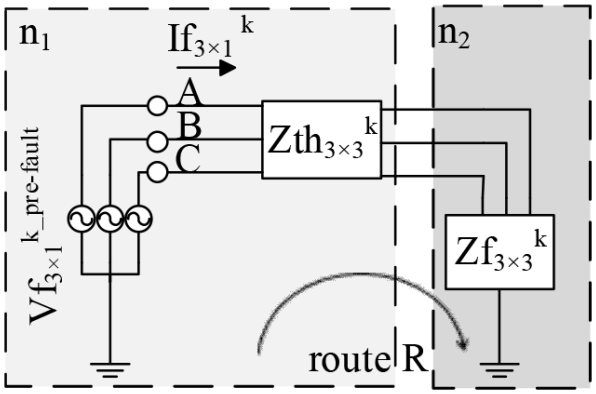

Figure 3. Thevenin's equivalent circuit of the fault condition.

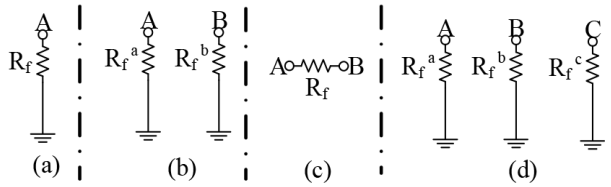

Figure 4. Thevenin's equivalent of the fault impedance: (a) single-phase-to-ground, (b) double-phase-to-ground, (c) phase-to-phase, (d) three-phase-to-ground.

$$\text{Single phase-to-ground } \rightarrow Zf = \begin{pmatrix} R_f & 0 & 0 \\ 0 & 0 & 0 \\ 0 & 0 & 0 \end{pmatrix} \quad ||\text{Double phase-to-ground} \rightarrow Zf = \begin{pmatrix} R_f^a & 0 & 0 \\ 0 & R_f^b & 0 \\ 0 & 0 & 0 \end{pmatrix}$$

$$\text{Phase-to-phase } \rightarrow Yf = \begin{pmatrix} \frac{1}{R_f} & -\frac{1}{R_f} & 0 \\ -\frac{1}{R_f} & \frac{1}{R_f} & 0 \\ 0 & 0 & 0 \end{pmatrix} ||\text{Three phase-to-ground } \rightarrow \ Zf = \begin{pmatrix} R_f^a & 0 & 0 \\ 0 & R_f^b & 0 \\ 0 & 0 & R_f^c \end{pmatrix} \tag{9}$$

$$\partial_k = norm(std(Zf_k^1, Zf_k^2, \cdots\cdots, Zf_k^m))^{-1}$$

$$where: \ Zf_k^m = \begin{pmatrix} R_f^a \\ R_f^b \\ R_f^c \end{pmatrix} \text{ or } \begin{pmatrix} R_f^a \\ R_f^b \end{pmatrix} or\,(R_f) \quad . \tag{10}$$

Accordingly, the maximum of ∂_k is a faulted bus with similar fault impedance. In one-, two-, and three-phase faults, Zf_{ik}^{im} has one, two, and three elements, respectively.

An auxiliary process has been used to improve the performance of the proposed method. This process detects infeasible solutions by analyzing the fault impedance. There are two groups of infeasible solutions. In the first group, the algorithm gives back negative resistance, whereas this is opposed by the first assumption (i.e. the fault has purely positive resistance). In the second group, the obtained results have unreasonable fault impedance. For example, during an AG fault, the algorithm detects fault impedance for healthy phases B and C. When fault impedances of each bus are included in the two above groups, ∂_k corresponding to the selected bus is equal to zero and it is removed from the results.

3. Simulation results

The proposed fault location scheme is evaluated in the IEEE 34-bus distribution system. The single-line diagram of the network is shown in Figure 5. The simulations are performed using PSCAD/EMTDC software. In PSCAD/EMTDC, a new component is created to provide the tightly coupled unbalanced distribution line. This proposed method is modified to be adaptable with different number of DG units or any change of the network's topology. These changes include changes in the placement or connecting/disconnecting of DG units, loads, or capacitor banks that should be considered in the modified three-phase impedance matrix.

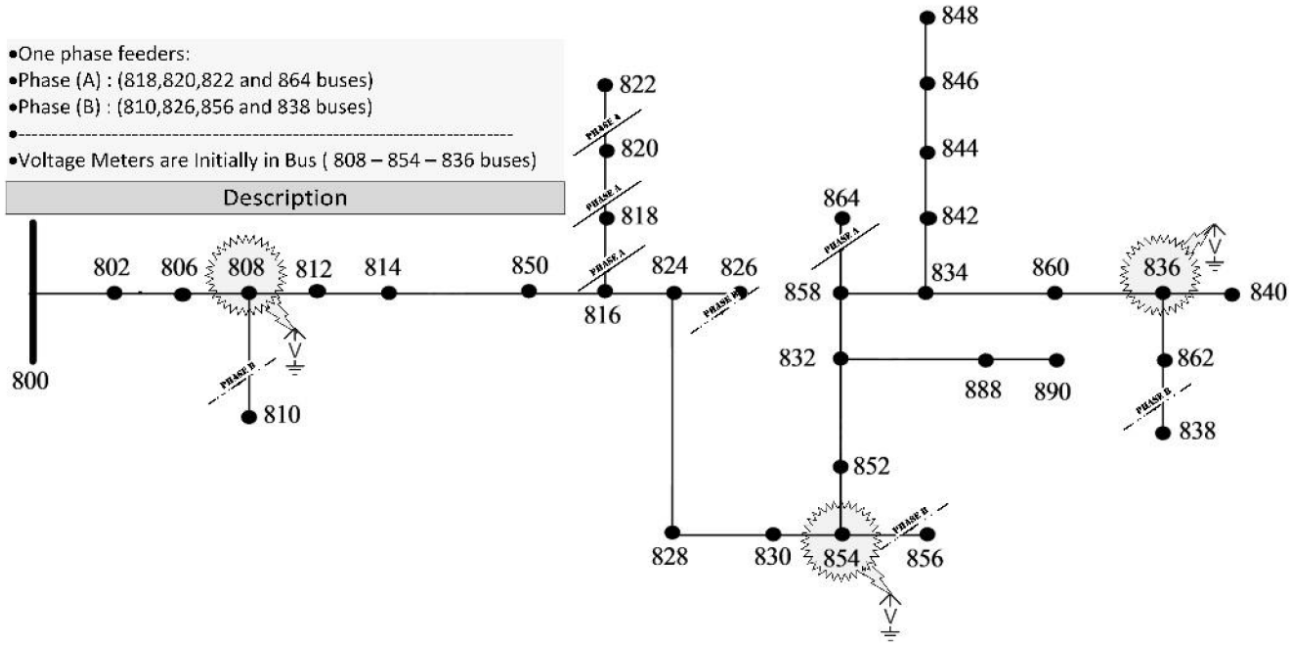

Figure 5. Single-line diagram of IEEE 34-bus distribution system.

Initially, these measurement devices are placed at buses 808, 854, and 836. In this paper, the proposed method is developed in a MATLAB environment that uses the measured data from PSCAD/EMTDC software to estimate the location of the fault.

The obtained numeric results corresponding to three types of faults, AG, BG, AB, and ABCG, are presented. It is worth noting that the achieved results from other types of faults are similar to the above-mentioned faults. The fault impedances are considered as purely resistance and they are arranged in low and high groups, 0.5 and 10 Ω, respectively. Moreover, it is assumed that the fault type has been already detected based on the proposed approach in [8].

In this paper, for the evaluation of numerical simulation results, at the beginning, all the error indexes are arranged in descending order of value. In the next step, if the second index is 90% or more of the first index, it demonstrates that the algorithm specifies the minimum two buses for the faulted bus. Therefore, the algorithm has multiple estimation; otherwise, it is assumed that the algorithm specifies only one faulted bus. Generally, the faults are simulated for each bus of the test case and the obtained results have been arranged into three classes: if the algorithm correctly recognizes the faulted bus, it will be categorized as the "success" class; when multiple buses consisting of faulted buses are specified, this situation will be categorized as "multiple"; and finally, the "fail" class will be used when the algorithm fails to find a faulted bus in the sample system.

3.1. Simulation results corresponding to PMUs

PMUs provide distributed measurements throughout the network. They are functionally available in protective relays, reclosers, and meters [21]. The obtained results are presented in Table 1 where the proposed fault location algorithm uses measured data from PMUs. Figure 6 demonstrates the measured data obtained from PMUs in PSCAD/EMTDC. All reported data are transmitted to the MATLAB environment as input of the algorithm based in Figure 1. From Table 1, the proposed method estimates the faulted bus successfully during all types of single-phase-to-ground fault. In this paper, three phase feeders and phase A of feeders (818, 820, 822, and 864 buses) will be tested under the AG fault and phase B of feeders (810, 826, 856, and 838 buses) is simulated under a phase B-to-ground (BG) fault. The proposed fault locator has acceptable performance when fault impedance changes from 0.5 to 10 Ω. There are eight single-phase feeders (phase B: 810, 826, 856, and 838; phase A: 818, 820, 822, and 864). According to the comparison between the obtained results for three-phase and double-phase faults in Table 1, the proposed method has acceptable results for different types of faults. For example, in the double-phase fault with 0.5 Ω resistance, the proposed method has 22 times success to locate the faulted bus, while in the three-phase fault with same resistance, the success results are 20. Therefore, the accuracy of the fault locator is reduced by about 8%. Moreover, in both situations, there is not any "fail" case.

Table 1. Simulation results of the proposed algorithm using both voltage magnitude and angle by PMUs.

Fault type / Result class	Single-phase-to-ground fault		Double-phase fault		Three-phase fault	
	Rf = 0.5 Ω	Rf = 10 Ω	Rf = 0.5 Ω	Rf = 10 Ω	Rf = 0.5 Ω	Rf = 10 Ω
Success	32	29	22	20	20	19
Multiple	2	5	4	6	6	6
Fail	0	0	0	0	0	1
No. of simulations	34	34	26	26	26	26

3.2. Simulation results corresponding to smart meters

Smart meters served as a distributed power quality measurement for the network. Increase of smart meters' implementation provides a profile of voltage sag in many points of a distribution system. In the proposed method, the magnitude of voltage deviation, which is measured by smart meters, is used. Neglecting the phase information of voltage sag causes a source of error in Eq. (4). Therefore, in this section, the performance of the proposed methodology is evaluated when the phase data are unavailable. Comparison between Tables 1 and 2 demonstrates that the accuracy of the proposed method is decreased, but the locator has acceptable performance.

Table 2. Simulation results of the proposed algorithm using voltage magnitude by smart meters.

Fault type / Result class	Single-phase-to-ground fault		Double-phase fault		Three-phase fault	
	Rf = 0.5 Ω	Rf = 10 Ω	Rf = 0.5 Ω	Rf = 10 Ω	Rf = 0.5 Ω	Rf = 10 Ω
Success	30	28	20	18	19	18
Multiple	4	6	6	8	7	7
Fail	0	0	0	0	0	1
No. of simulations	34	34	26	26	26	26

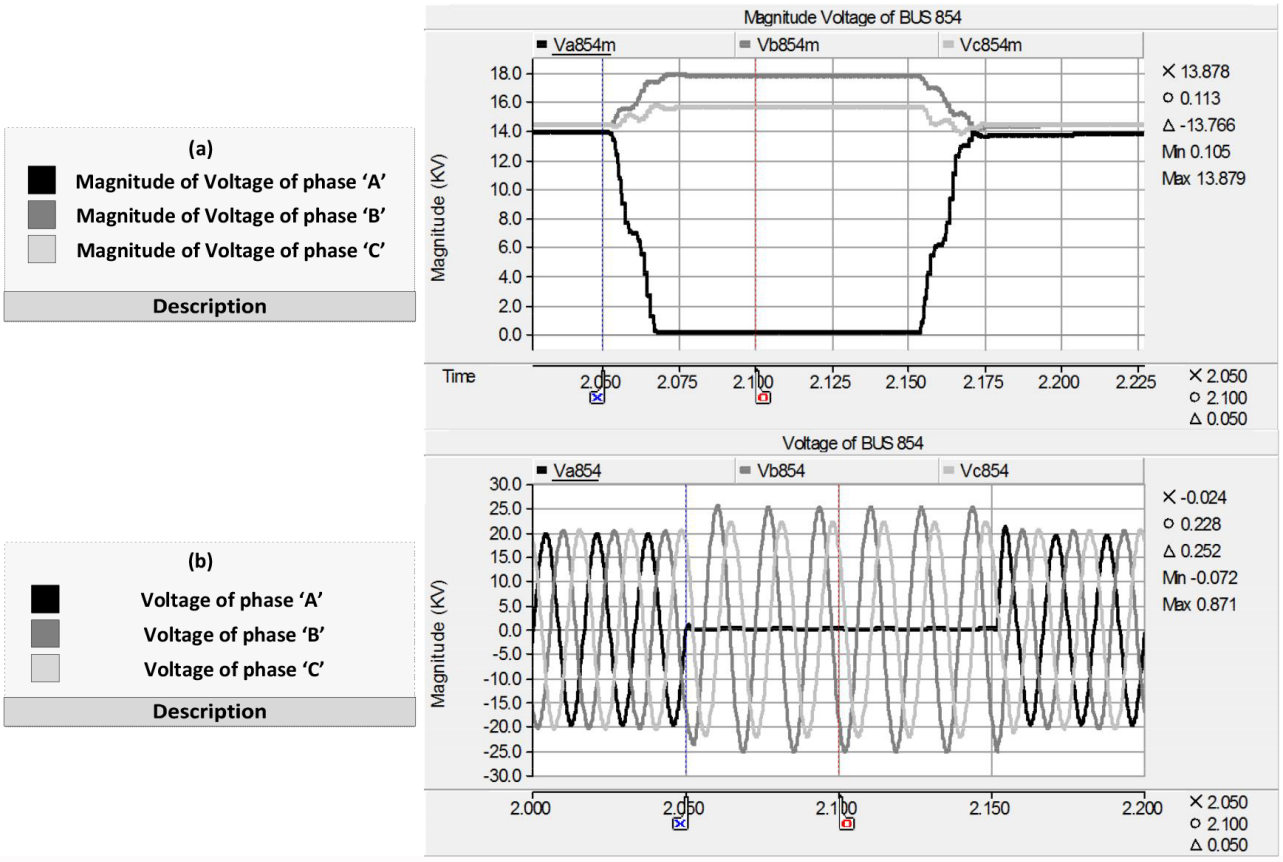

Figure 6. Report of PMUs located at bus 854 when bus 82 is under AG-fault condition at 2.05 s: (a) magnitude of three-phase voltage signals, (b) three-phase voltage signals.

3.3. Impact of measurement noise

System unbalances, measurement hardware error, line loading variations, etc. cause system noise and frequency inconstancy that will affect the fault locator accuracy [22]. The accuracy of smart meters of a feeder is usually in the range of 0.1%–0.5% [23]. In this paper, noise is considered as a normal distribution of zero mean, μ, and 1% of standard deviation, σ. Noise is considered by multiplication of both magnitude and phase of measurement in (n+1) where 'n' is the number that is generated by normal distribution [11]. Table 3 shows the robustness of obtained simulation results while each PMU has noise N (0, 1%).

Figure 7 displays the error index of the faulted bus, 828, without and with noise conditions. These error

Table 3. Simulation results of the proposed algorithm by PMUs with noise generated from n (0, 1%).

Fault type / Result class	Single-phase-to-ground fault		Double-phase fault		Three-phase fault	
	Rf = 0.5 Ω	Rf = 10 Ω	Rf = 0.5 Ω	Rf = 10 Ω	Rf = 0.5 Ω	Rf = 10 Ω
Success	30	28	21	19	18	19
Multiple	4	6	5	7	8	6
Fail	0	0	0	0	0	1
No. of simulations	34	34	26	26	26	26

indexes are the output of the fault detection algorithm that is calculated according to Eq. (10). Moreover, the auxiliary process assists the algorithm to improve the results. In Figure 7, it is obvious that the faulted bus is recognized distinctively. In the situation without noise, the proposed method finds the faulted bus in all cases. Furthermore, the suggested methodology has acceptable performance even in noisy conditions.

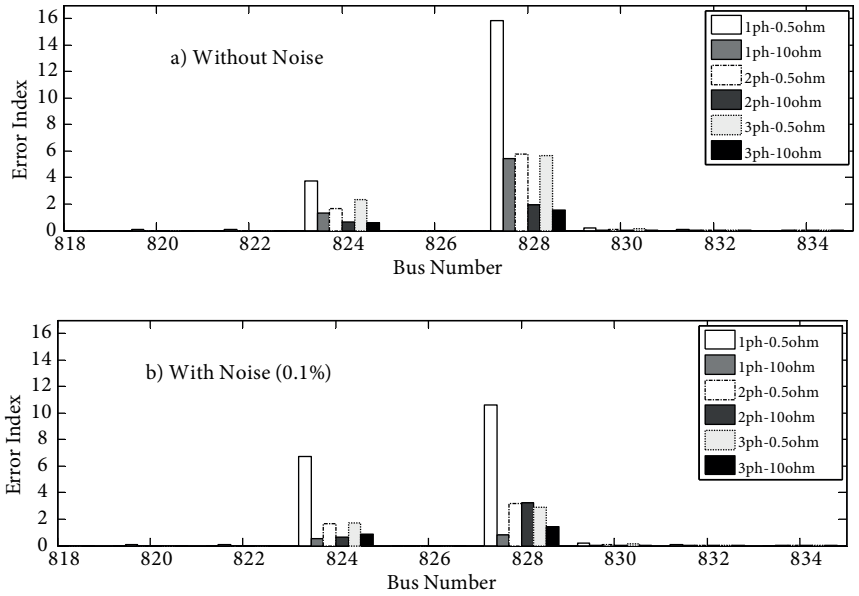

Figure 7. Error index for bus 828: (a) without noise, (b) with noise (0, 1%).

3.4. Impact of location of measurement devices

In this section, two cases are considered to demonstrate the influence of the measurement device placement in the fault location results:

Case 1) PMUs installed at buses 806-828-852

Case 2) PMUs installed at buses 840-836-858

In the first case, the placements of PMUs are changed. In the second case, all devices are lumped into a region. From Table 4, when PMUs are compacted in one region, the accuracy of the obtained results is decreased considerably.

Table 4. Impact of feeder meter allocation.

Fault type / Result class	Single-phase-to-ground fault		Double-phase fault	
	Case 1	Case 2	Case 1	Case 2
Success	26	22	19	15
Multiple	7	9	6	9
Fail	1	3	1	2
No. of simulations	34	34	26	26

According to Eq. (4), when two buses have nearly mutual impedance, they have close fault currents, too, and it is hard to determine the faulted bus between them. Figure 8 shows how mutual impedance changes for two selected buses, 808 and 836 (on the horizontal axis of Figures 8a and 8b, number 1 is bus 800 and 34 is bus 834). In Figures 8a and 8b, the first three mutual impedances are mutual impedances of bus 800, 802,

and 806, respectively. It can be observed from Figure 8a that this mutual impedance is greater than in Figure 8b. In other words, mutual impedance depends on the location of the calculation. Whatever the increase of distance between selected buses, the mutual impedance of the measured bus is decreased. That is the main reason why the number of "multiple" and "fail" cases of the proposed algorithm increases considerably when all of the PMUs are lumped in one region.

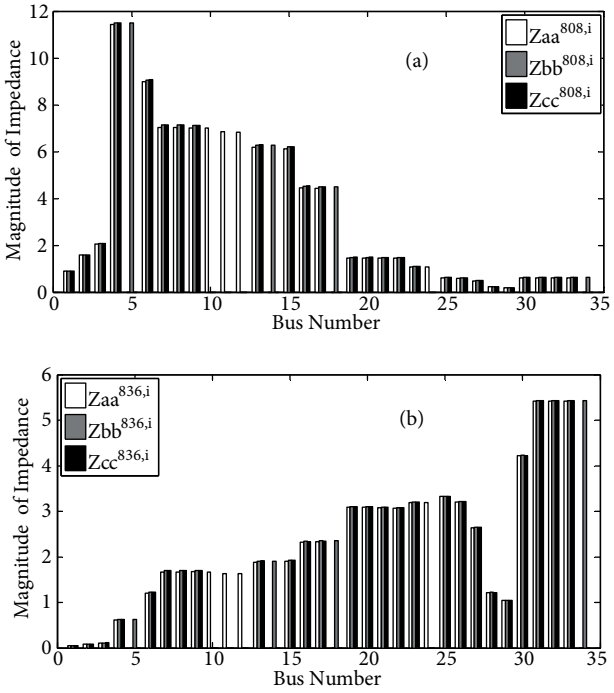

Figure 8. Mutual impedance: (a) bus 808, (b) bus 836.

3.5. Impact of load estimate accuracy

Although load impedance calculations are described in Section 2, exact load impedance is scarcely achieved in a real distribution system. There is a certain degree of uncertainty, especially in the load impedance, that should be considered in fault location problems. In this section, the effect of load uncertainty on the performance of the proposed method is investigated. The load uncertainties are defined by addition of an average 20% variation in the load impedance [13]. In Table 5, the impact of load impedance uncertainty on the performance of the proposed method is negligible.

Table 5. Impact of load value estimation errors.

Fault type / Result class	Single-phase-to-ground fault			Double-phase fault		
	Value of load impedance uncertainty					
	–20%	0%	+20%	–20%	0%	+20%
Success	32	32	31	20	22	22
Multiple	2	2	3	6	4	4
Fail	0	0	0	0	0	0
No. of simulations	34	34	34	26	26	26

4. Discussion and comparison

In this section, the proposed method will be compared with previous similar studies from two viewpoints: modeling of the case study and the performance of the algorithm.

4.1. Modeling

In [11,13,15], only three-phase feeders were considered, but in this paper, the proposed methodology is tested on the IEEE 34-bus distribution system, which has eight single-phase feeders. By considering the single-phase feeders, the heterogeneous lines as a challenging issue of fault location in distribution systems are included in the proposed algorithm. Single-phase feeders increase the complexity of locating faults based on an impedance matrix because the mutual impedance matrix is a singular one.

In [11,16], the effects of loads have been ignored in the three-phase impedance matrix. However, the loading levels in the distribution systems are smaller than in the transmission systems, but ignoring them is a source of error. The impact of neglecting loads in the impedance matrix was explained in [13]. In the proposed method, six different types of load are considered in the IEEE 34-bus distribution system and they are included in the impedance matrix as described in Section 2.

4.2. Performance

In [15], load uncertainty affected the obtained accuracy results. In addition, an iterating method that calculates backward/forward load flow at each node was used. It has high computational effort and convergence challenges. In this paper, simulations are executed in a system with Intel core i3 2.4 GHz CPU and 4 GB RAM. The average run-time of the fault location algorithm is about 0.3 s in the MATLAB environment.

In [16], the proposed method estimated the fault current using the sum of all the phasors of the injected currents into the system. Injected current calculation uses synchronized measurements of current at each distributed generator node. The voltage sag is then compared with the measured voltage sag calculated from Eq. (3). This method needs synchronized measurements of both current and voltage in interconnection of DG units that increase the implementation cost. In this paper, the proposed method uses them only in root node. Moreover, in [16], there was no sensitivity analysis.

In [13], the proposed method was implemented in the IEEE 34-bus distribution system and Table 6 demonstrates the results of proposed methods in [13] and this paper. In this paper, the former equations in [13] are improved to achieve more accurate results. This confirms that the proposed fault locator has better performance to locate a fault in the network. For example, in the single-phase-to-ground fault with 0.5 Ω resistance, the proposed method of this paper has 94% success to locate a fault but another algorithm has success of about 76%. Moreover, both the methods locate the faulted bus without any failures. In the double-phase fault with 0.5 Ω resistance, the proposed method of this paper has 84% success without any failure to locate a fault, but the method in [13] has one failure and it has 69% success to locate a fault.

Table 6. Compression between proposed algorithm and method in [13].

Fault type / Result class	Single-phase-to-ground fault		Double-phase fault	
	This paper	[13]	This paper	[13]
Success	32	26	22	18
Multiple	2	8	4	7
Fail	0	0	0	1
No. of simulations	34	34	26	26

5. Conclusion

Fault location based on the similarity of fault impedance has been introduced in this paper. A three-phase impedance matrix and voltage measurement are utilized to locate a fault in the distribution system. Since this method uses only voltage sag measurement, it is easy to apply in a real system. Unbalanced lines, loads, and distributed generators are modeled in the proposed method. Sensitivity analyses demonstrate that the proposed method has good performance at different noise levels, fault resistances, fault types, and numbers of measurements. The method is capable of being used in conventional distribution systems because it has acceptable performance when the number of meters is decreased as well as using smart meters instead of PMUs. In this paper, the meters are randomly placed in the network while the location of metering devices affects the performance of the method. It is one of the main topics related to the proposed method that optimizes the location of meters and quantity in future studies.

References

[1] Janssen P. Monitoring, protection and fault location in power distribution networks using system. PhD, University of Brussels, Belgium, 2014.

[2] Kezunovic M. Smart fault location for smart grids. IEEE T Smart Grid 2011; 2: 11-17.

[3] Alwash SF, Ramachandaramurthy VK. New impedance-based fault location method for unbalanced power distribution systems. INT T Electr Energy 2015; 25: 1008-1021.

[4] Ren J, Venkata SS, Sortomme E. An accurate synchrophasor based fault location method for emerging distribution systems. IEEE T Power Deliver 2014; 29: 297-298.

[5] Liang R, Wang F, Fu G, Xue X, Zhou R. A general fault location method in complex power grid based on wide-area traveling wave data acquisition. Int J Elec Power 2016 31; 83: 213-218.

[6] He Z, Li X, Chen S. A traveling wave natural frequency-based single-ended fault location method with unknown equivalent system impedance. Int T Electr Energy 2016; 26: 509-524.

[7] Dong Y, Zheng C, Kezunovic M. Enhancing accuracy while reducing computation complexity for voltage-sag-based distribution fault location. IEEE T Power Deliver 2013; 28: 1202-1212.

[8] Jiang H, Zhang JJ, Gao W, Wu Z. Fault detection, identification, and location in smart grid based on data-driven computational methods. IEEE T Smart Grid 2014; 5: 2947-2956.

[9] Lotfifard S, Kezunovic M, Mousavi MJ. A systematic approach for ranking distribution systems fault location algorithms and eliminating false estimates. IEEE T Power Deliver 2013; 28: 285-293.

[10] Mokhlis H, Awalin LJ, Bakar AHA, Illias HA. Fault location estimation method by considering measurement error for distribution networks. Int T Electr Energy 2014; 24: 1244-1262.

[11] Majidi M, Arabali A, Etezadi-Amoli M. Fault location in distribution networks by compressive sensing. IEEE T Power Deliver 2015; 30: 1761-1769.

[12] Majidi M, Etezadi Amoli M, Sami Fadali M. A novel method for single and simultaneous fault location in distribution networks. IEEE T Power Deliver 2015; 30: 3368-3376.

[13] Trindade FCL, Freitas W, Vieira JCM. Fault location in distribution systems based on smart feeder meters. IEEE T Power Deliver 2014; 29: 251-260.

[14] Cheng CS, Shirmohammadi D. A three-phase power flow method for real-time distribution system analysis. IEEE T Power Syst 1995; 10: 671-679.

[15] Pereira RF, da Silva LGW, Kezunovic M, Mantovani JRS. Improved fault location on distribution feeders based on matching during-fault voltage sags. IEEE T Power Deliver 2009; 24: 852-862.

[16] Brahma SM. Fault location in power distribution system with penetration of distributed generation. IEEE T Power Deliver 2011; 26: 1545-1553.

[17] Barker PP, De Mello RW. Determining the impact of distributed generation on power systems In: Power Engineering Society Summer Meeting; 16–20 July 2000; Seattle, WA, USA. New York, NY, USA: IEEE. pp. 1645-1656.

[18] Kersting WH. Distribution System Modeling and Analysis. Boca Raton, FL, USA: CRC Press, 2008.

[19] Makram EB, Girgis AA. A generalized computer technique for the development of the three-phase impedance matrix for unbalanced power systems. Electr Pow Syst Res 1988; 15: 41-50.

[20] Grainger JJ, Stevenson W Jr. Power System Analysis. New York, NY, USA: McGraw-Hill, 1994.

[21] Bower W, Ton D, Guttromson R, Glover S, Stamp J, Bhatnagar D, Reilly J. The Advanced Microgrid Integration and Interoperability. Sandia Report. Albuquerque, NM, USA: Sandia National Laboratories, 2014.

[22] Jiang J, Yang J, Lin Y, Liu C, Ma J. An adaptive PMU based fault detection/location technique for transmission lines. I. Theory and algorithms. IEEE T Power Deliver 2000;15: 486-493.

[23] IEEE. Standard for Synchrophasor Measurements for Power Systems, IEEE Std. C37.118.1-2011 (Revision of IEEE Std. C37.118-2005). New York, NY, USA: IEEE, 2011.